Rossby Waves in Opposing Currents

BRIAN FARRELL AND IAN WATTERSON

Center for Earth and Planetary Physics, Harvard University, Cambridge, MA 02138

(Manuscript received 24 September 1984, in final form 1 April 1985)

ABSTRACT

A barotropic Rossby wave incident to a region of increasing mean flow velocity opposing the wave group velocity undergoes a reversal of direction at a stopping point where the mean flow velocity and local wave group velocities are equal and opposite. Incident wave amplitude increases approaching this stopping point, which may be referred to as a group velocity critical layer, but eventually suffers a decrease along its trajectory so that the reflected wave amplitude and energy tend to zero on approach to a phase velocity critical layer located where the opposing flow vanishes.

Some applications of this process to observations of synoptic scale Rossby waves are suggested and an example of the interaction of an incident wave with a barotropic model of the Hadley circulation is presented to illustrate these ideas.

1. Introduction

The phenomenon of absorption of Rossby waves at a critical level where the zonal phase velocity is equal to the zonal mean velocity has been widely studied (Dickinson, 1968; Tung, 1979). This critical level absorption in the linear viscous problem has been invoked to explain the observed inability of midlatitude topographic Rossby waves to penetrate the tropical easterly trade winds. There is currently an unresolved question concerning the influence of nonlinearity on critical layers leading to possible reflection rather than absorption (Geisler and Dickinson, 1974), but this will not concern us here. Instead we will retain the linear approximation and show that waves propagating into an adverse mean current are reflected by the opposing flow and absorbed by Reynold's stress interaction with the mean along a trajectory that eventually ends at a critical level. Such reflection could, for instance, prevent midlatitude Rossby waves from reaching the zonal wind critical level and result instead in absorption near the northern terminus of the Hadley circulation.

The analysis uses ray tracing completed by patching at the stopping point. It closely parallels that for the hydraulic breakwater problem of surface water waves (Smith, 1976; Peregrine and Smith, 1979). It turns out to be similar as well to the situation arising from Rossby waves propagating in a zonal direction through sheared meridional flow where the same progression of the wave through its eventual critical level precedes reflection at the stopping point. The study of that situation arises from Rossby waves incident from midocean onto western boundary currents. (Yamagata, 1976; Geisler and Dickinson, 1976). The increase in amplitude of easterly waves in opposing currents has been studied in the context of the genesis of hurricanes (Shapiro, 1977).

2. Analysis

The linearized barotropic potential vorticity equation on a β-plane is

$$\left(\frac{\partial}{\partial t} + \bar{U}(x, y)\frac{\partial}{\partial x} + \bar{V}(x, y)\frac{\partial}{\partial y}\right)\nabla^2\psi + (-\psi_y\bar{q}_x + \psi_x q_y + \nabla^2\psi\nabla\cdot\bar{\mathbf{V}}) = 0, \quad (1)$$

where

t time
x zonal distance
y meridional distance
$\bar{U}$ zonal basic state velocity
$\bar{V}$ meridional basic state velocity
$\bar{\mathbf{V}}$ $(\bar{U}, \bar{V})$
$\bar{q}$ $(\bar{V}_x - \bar{U}_y) + f_0 + \beta y$ basic state potential vorticity
ψ perturbation streamfunction.

For simplicity we will assume a divergent mean flow of the form $[\bar{U}(x), \bar{V}(y)]$ and a scale separation

$$\mu = \frac{\text{length scale of perturbations}}{\text{length scale of basic state}} \ll 1$$

which allows (1) to be written at order μ as

$$\left(\frac{\partial}{\partial t} + \bar{U}\frac{\partial}{\partial x} + \bar{V}\frac{\partial}{\partial y}\right)\nabla^2\psi + \beta\psi_x = -\mu\nabla^2\psi\nabla\cdot\bar{\mathbf{V}}. \quad (2)$$

Substituting the solution form $\psi = a\exp[i(kx + ly - \omega t)]$ in (2) gives at order μ^0

$$G(\omega, k, l, x, y, t)a\exp[i(kx + ly - \omega t)] = 0,$$

where

$$G = \omega - \bar{U}k - \bar{V}l + \frac{\beta k}{k^2 + l^2} = 0 \qquad (3)$$

is the dispersion relation.

Consider first the zonal case $\bar{U} = \bar{U}(x)$, $\bar{V} = 0$ for which (3) becomes

$$G = \omega - \bar{U}(x)k + \frac{\beta k}{k^2 + l^2} = 0. \qquad (4)$$

We imagine exciting a wave far from the stopping point with a forcing frequency ω. If the opposing current increases in the direction of wave propagation a stopping point is eventually reached where the zonal flow is equal in magnitude to C_g the local group velocity

$$\frac{\partial \omega}{\partial k} = \bar{U} + \frac{\beta(k^2 - l^2)}{(k^2 + l^2)^2} = 0.$$

At order μ in (2) we find that both incident and reflected waves have amplitude given by the conservation of wave action flux (Young and Rhines, 1980):

$$B_0 = (\bar{U} + C_g)A$$

$$= \left[\bar{U} + \frac{\beta(k^2 - l^2)}{(k^2 + l^2)^2}\right]\left[-\frac{1}{4}\frac{(k^2 + l^2)^2}{\beta k}a^2\right], \qquad (5)$$

where

$$A = \frac{E}{\hat{\omega}} = -\frac{1}{4}\frac{(k^2 + l^2)^2 a^2}{\beta k}$$

is the wave action density, $\hat{\omega} = -\beta k/(k^2 + l^2)$ is the local frequency and E the energy density.

The first term on the right-hand side of (5) goes to zero at the stopping point and as the second is nonsingular in k and l, the amplitude rises indefinitely in this ray approximation. At the same time the wavenumber along the trajectory is determined by the kinematic relation (Lighthill, 1978):

$$l = l_0$$

$$\frac{dk}{dt} = -k\frac{\partial \bar{U}}{\partial x}.$$

The zonal wavenumber increases monotonically for propagation into an opposing current with variation along the path:

$$\frac{dk}{dx} = \frac{1}{dx/dt}\frac{dk}{dt} = \frac{-k\bar{U}_x}{(\bar{U} + C_g)}.$$

We see that dk/dx becomes infinite at the stopping point. For Rossby waves on final approach to the phase velocity critical level $\bar{U} = 0$, we find below that $k \to \infty$ as well so that this line is characterized by $C_g \to 0$, $k \to \infty$ and is properly a critical level. The stopping point in contrast is not a singular point of the equations and k varies smoothly there in the complete solution although the ray tracing solution has a singular derivative at this point. The wave amplitude vanishes on approach to the phase velocity critical level as the limit of (5) when $\bar{U} \to 0$, $k \to \infty$ is $B_0 = -ka^2/4$.

Rossby wave trajectories in convergent zonal flows divide naturally into two cases: those for which $C_g > 0$ and the stopping point lies to the east of the wave source and those with $C_g < 0$ for which the stopping point lies to the west. We begin the analysis for the constant convergence $\bar{U}_x = -s$ by nondimensionalizing (4)

$$t' = st$$

$$(x', y') = \frac{\beta}{s}(x, y)$$

and applying the additional scaling $\tilde{k} = k'/k'_0$, $\tilde{x} = x'k'^2_0$, where the subscript 0 refers to the phase velocity critical level taken to lie at $x = 0$. The dispersion relation is then

$$-\frac{1}{1 + \alpha^2} + \tilde{x}\tilde{k} + \frac{\tilde{k}}{\tilde{k}^2 + \alpha^2} = 0$$

and has only $\alpha \equiv l'_0/k'_0$ as a free parameter.

An example of eastward propagation is obtained by setting $\alpha = 0$ and the resulting trajectory in $(\tilde{x}, \tilde{k})$ space is shown in Fig. 1. The wave is excited at $\tilde{x}_E = -0.25$, passes through the critical level at $\tilde{x}_{CL} = 0$ to reach its stopping point at $\tilde{x}_{SP} = 0.25$, is reflected and eventually absorbed on approach to the critical level. The amplitude from (5) is indicated by the dashed line and is seen to diverge at the stopping point before approaching zero along the reflected trajectory. It is clear that ray theory breaks down in the immediate vicinity of the stopping point.

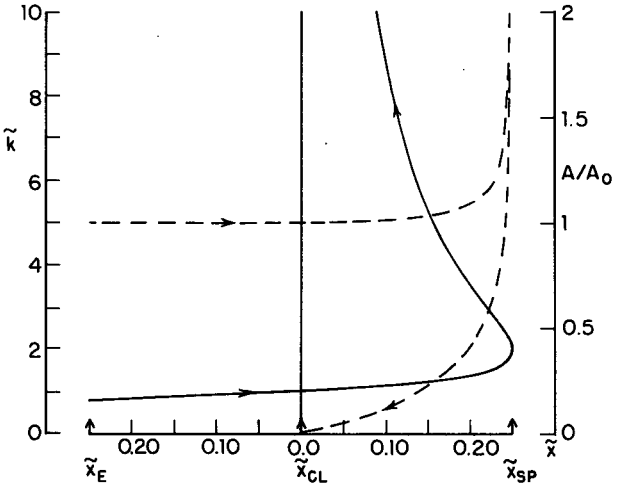

FIG. 1. Trajectory of an eastward propagating Rossby wave in the convergent zonal flow $\bar{U}_x = -s$. The solid line is the nondimensional zonal wavenumber $\tilde{k}$ and the dashed line is the amplitude A/A_0 normalized to its value at the critical level. Arrows indicate the direction of propagation from the excitation latitude $\tilde{x}_E$ to the stopping point $\tilde{x}_{SP}$ where the wave is reflected back to the critical level $\tilde{x}_{CL}$.

An example of westward propagation is obtained by the choice $\alpha = 4.0$ and is shown in Fig. 2. The wave excited at $\tilde{x}_E = 0.02$ reaches a stopping point at $\tilde{x}_{SP} = -0.021$, is reflected and passes again through $\tilde{x}_{CL} = 0$ before being reflected a second time and finally reaching its critical level. The second singularity in the ray solution occurs at very high wavenumber and, although amenable to the same analysis as the first, is probably not of physical significance.

The inability of Rossby waves to penetrate opposing currents results from two simultaneous effects: the increase in the opposing current along the path and the decrease in the local group velocity as the wave propagates along its trajectory of ever increasing k. For $\beta = 1.6 \times 10^{-11}$ m^{-1} s^{-1}, $s = -5$ cm s$^{-1}/10^3$ km and $k = 2\pi/10^3$ km, the stopping point in the first example occurs at $x = 2 \times 10^3$ km and the penetration will be even less for higher values of s. This extreme vulnerability of Rossby waves to opposing currents must call into question the validity of WKB analysis for some realistic flows. However, the examples to follow will vindicate our qualitative predictions.

The trajectory in physical (x, y) space for the second example is found by using the meridional group velocity $C_{gy} = (2\beta kl)/(k^2 + l^2)^2$ to complete the ray path. In particular, the wave approaches its critical level at normal incidence. Alternatively and perhaps of more relevance to geophysical jets, the meridional structure may be interpreted as of modal form resulting, for instance, from confinement in a channel so that there is no net propagation in y.

To complete the description of Rossby waves in opposing zonal currents, we need to find the solution near the stopping point. At this point, here taken as $x_{sp} = 0$, the dispersion relation may be approximated:

$$G(x, k) = xG_x|_{xSP=0} + \frac{1}{2}(k - k_{SP})^2 G_{kk}|_{kSP} + \cdots = 0,$$

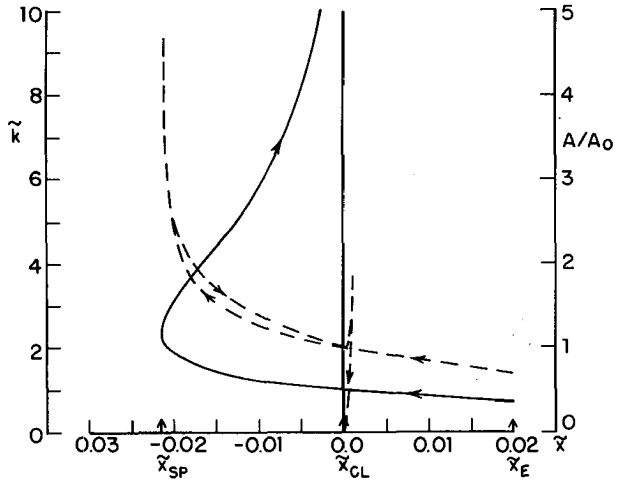

FIG. 2. As in Fig. 1 except for the westward traveling wave with $\alpha = 4.0$.

where

$$G_x = -\bar{U}_x k, \quad G_{kk} = \beta k(2k^2 - 6l^2)/(k^2 + l^2)^3. \quad (6)$$

The wavenumber just away from the stopping point is

$$k = k_{SP} \pm \left(\frac{2G_x}{G_{kk}}\right)^{1/2} (-x)^{1/2} \quad (7)$$

from which (5) gives the amplitude

$$a \approx \left(\frac{B_0^2}{2G_xG_{kk}}\right)_{kSP}^{1/4} \frac{(-x)^{-1/4}}{(k_{SP}^2 + l^2)/(4\beta k_{SP})^{1/2}}. \quad (8)$$

The incoming wave is on the negative branch of (7), while the outgoing is on the positive consistent with k increasing along the ray path. The solution just away from the stopping point is

$$\begin{aligned}\psi &= \left(\frac{B_0^2}{2G_xG_{kk}}\right)^{1/4} \frac{(-x)^{-1/4}}{(k_{SP}^2 + l^2)/(4\beta k_{SP})^{1/2}} \\ &\quad \times \exp[i(k_{SP}x - \omega_0 t)] \\ &\quad \times \left\{\exp\left[\left(i\frac{2G_x}{G_{kk}}\right)_{kSP}^{1/2} \int (-x)^{1/2} dx\right]\right. \\ &\quad \left. - \exp\left[-i\left(\frac{2G_x}{G_{kk}}\right)_{kSP}^{1/2} \int (-x)^{1/2} dx\right]\right\} \\ &= 2\left(\frac{B_0^2}{2G_xG_{kk}}\right)^{1/4} \frac{(-x)^{-1/4}}{(k^2 + l^2)/(4\beta k_{SP})^{1/2}} \\ &\quad \times \exp[i(k_{SP}x - \omega_0 t)] \\ &\quad \times \sin\left[\frac{2}{3}\left(\frac{2G_x}{G_{kk}}\right)^{1/2} (-x)^{3/2} + \frac{\pi}{4}\right]. \quad (9)\end{aligned}$$

The undetermined phases have been chosen with foresight to give the sine behavior.

We are now ready to find the inner solution. The linear equation is identified with its Fourier transform

$$G(\omega, k, x)a(x)e^{i\chi} = 0, \quad (10)$$

where $\chi = kx - \omega t$ contains the rapidly varying phase and $a(x)$ is assumed to vary on a longer scale. Taking advantage of the scale separation, (10) may be written near $\chi_{SP} = 0$ as

$$G\left(\omega_{SP}, k_{SP} - i\frac{\partial}{\partial x}, x\right)a(x)e^{ix_{SP}} = 0.$$

Using the local dispersion relation to isolate the slow space scale and Taylor expanding about $x_{SP} = 0$ yields:

$$Ga - iG_k\frac{\partial a}{\partial x} + xG_x a - \frac{1}{2}G_{kk}\frac{\partial^2 a}{\partial x^2} + \cdots = 0$$

but $G = G_k = 0$ at x_{SP} so this reduces to an Airy equation for the amplitude variation

$$xG_x a - \frac{1}{2}G_{kk}\frac{\partial^2 a}{\partial x^2} = 0 \quad (11)$$

with solution

$$a = A_0 A_i\left[\left(\frac{2G_x}{G_{kk}}\right)^{1/3} x\right].$$

To recap, the rapid phase variations satisfy the local dispersion relation at the stopping point but the amplitude is modulated on a longer space scale by the solution to (11) which arises from the leading order variation of the local dispersion at this point.

To find A_0 we must match the outer solution (9) using the asymptotic formula for A_i at large negative argument

$$A_i(\gamma) \approx -\frac{1}{\sqrt{\pi}}\frac{1}{(-\gamma)^{1/4}}\left[\frac{2}{3}(-\gamma)^{3/2} + \frac{\pi}{4}\right].$$

Substituting for γ we find that our choice of phases in (9) was correct and that the amplitude is

$$A_0 = -\frac{\sqrt{B_0}}{(k_{SP}^2 + l^2)/(4\beta k_{SP})^{1/2}}\left(\frac{32\pi^3}{G_{kk}^2 G_x}\right)_{SP}^{1/6}$$

from which it is seen that modifying the flow changes the maximum amplitude at the stopping point only as $G_x^{-1/6} = (-\bar{U}_x k_{SP})^{-1/6}$.

It is tempting to speculate that a large amplitude would be obtained when $G_{kk} = 0$ which occurs for $k_{SP} = \sqrt{3}l$. This triple point caustic (Smith, 1976) differs from the stopping point examined above in that the trajectory passes through the singular region rather than being reflected. An example of such a trajectory for which $k_0 \equiv k_{SP} = \sqrt{3}/2$ and $l_0 = 1/2$ is shown in Fig. 3. The amplitude near the triple point can be found by using the third order analogue of the Airy equation.

Although the ray tracing solution predicts a maximum, in fact infinite, wave amplitude at the stopping point, the Airy solution has its maximum $A_i(\gamma) = 0.53565$ at $\gamma = -1.01879$ considerably on the wave side of the stopping point and the maximum amplitude reached in the Airy solution is in most cases quite modest. The ratio R of the amplitude of the incoming wave at $x = 0$ to the maximum achieved by the Airy solution is

$$R = 0.53565\left[32\pi^3 \frac{\beta}{|s|k_0}\frac{(k_0^2 - l^2)^3}{k_0^2(2k_{SP}^2 - 6l^2)^2}\right]^{1/6}.$$

For the example in Fig. 1, this yields

$$R = 0.85\left(\frac{\beta}{|s|k_0}\right)^{1/6};$$

if we take the values used previously; $\beta = 1.6 \times 10^{-11}$ m^{-1} s^{-1}, $s = -5$ cm s^{-1}/10^3 km, $k_0 = 2\pi/10^3$ km we find $R = 1.64$.

The qualitative picture which emerges is that a Rossby wave entering a region of convergent zonal velocity would be observed to increase in amplitude coincident with a decrease in zonal wavelength, reach a maximum of amplitude when its wavelength has been reduced to approximately half its original value and continue to steepen as its amplitude falls. This steepening occurs because the wavenumber increases more rapidly than the amplitude decreases, steepness being the product of these quantities and equal in magnitude to the meridional velocity. Steepness increase (by a factor of 8.3 at $\tilde{x} = -0.1$ in Fig. 2) must eventually give rise to secondary development and observations (Holopainen and Rontu, 1981; Palmen and Newton, 1969, p. 276) suggest this results ultimately in the formation of cutoffs.

Turning to the case of constant zonal flow and an opposing meridional current, the dispersion relation (4) becomes

$$G = \omega - \bar{U}k - \bar{V}(y)l + \frac{\beta k}{k^2 + l^2} = 0, \qquad (12)$$

and the condition for a stopping point is

$$\bar{V} + \frac{2\beta k l}{(k^2 + l^2)^2} = 0.$$

Wave action flux is not conserved in this case (Young and Rhines, 1980) as the meridional velocity divergence serves as a source of action. However, it can be shown that for a wave excited at $y = y_E$ the quantity

$$A' = A \exp\left(\int_{y_E}^{y} \frac{\bar{V}_y}{\bar{V} + C_g}\, dy\right)$$

has nondivergent flux so that the following is constant along the trajectory

$$B_0 = \left(\bar{V} + \frac{2\beta k l}{(k^2 + l^2)^2}\right)\left(-\frac{1}{4}\frac{(k^2 + l^2)^2}{\beta k} a^2\right) \times \exp\left[\int_{y_E}^{y} \frac{V_y dy}{\bar{V} + (2\beta k l/(k^2 + l^2)^2)}\right] \qquad (13)$$

from which we may find the amplitude, a. While the

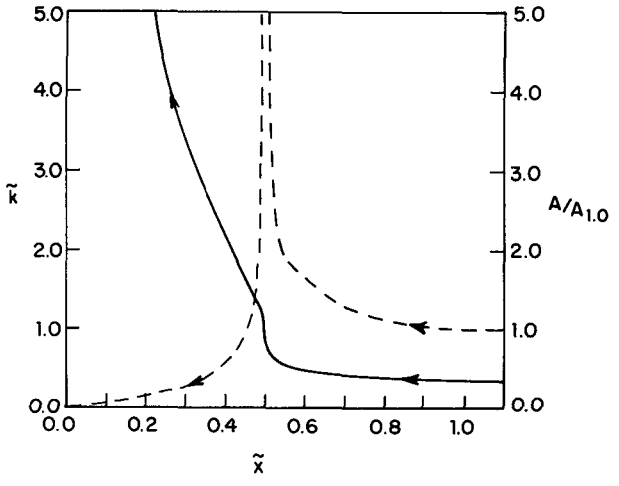

FIG. 3. The triple point caustic with $k_{SP} = \sqrt{3}/2$ and $l_0 = 1/2$.

zonal wavenumber is constant, $k = k_0$, the meridional wavenumber is given by the kinematic condition

$$\frac{dl}{dt} = -l\frac{\partial \bar{V}}{\partial y}$$

and increases along the trajectory as before; by similar argument $a \to 0$, $l \to \infty$ at the phase velocity critical level, $\bar{V} = 0$.

The dispersion relation (12) is nondimensionalized, as before, and the additional scaling $\tilde{l} = l'/k_0'$, $\tilde{y} = y'k_0'^2$, $\alpha = l_0'/k_0'$ reduces it with $\bar{V} = -sy$ to

$$\frac{-1}{1+\alpha^2} + \tilde{y}\tilde{l} + \frac{1}{1+\tilde{l}^2} = 0.$$

As an example of a Rossby wave in an opposing meridional current, we set $k_0' = 1.0$, $l_0' = -1.0$. The resulting trajectory is shown in Fig. 4, together with the amplitude from (13). The wave is excited at $\tilde{y}_E = 0.05$, reaches a stopping point at $\tilde{y}_{SP} = -0.15$ and then is reflected and eventually absorbed on approach to the critical level $\tilde{y}_{CL} = 0$. The trajectory in physical space may be found by including the zonal group velocity $C_{gx} = [\beta(k^2 - l^2)]/[(k^2 + l^2)^2]$.

The Airy function patching proceeds by replacing

$$x \to y$$
$$k \to l$$
$$G_y = -\bar{V}_y l$$
$$G_{ll} = 2\beta k \frac{3l^2 - k^2}{(k^2 + l^2)^3}.$$

The amplitude variation near the stopping point is controlled by the $(\bar{V} + C_g)$ term in (13); it is not affected by the additional variation in A'.

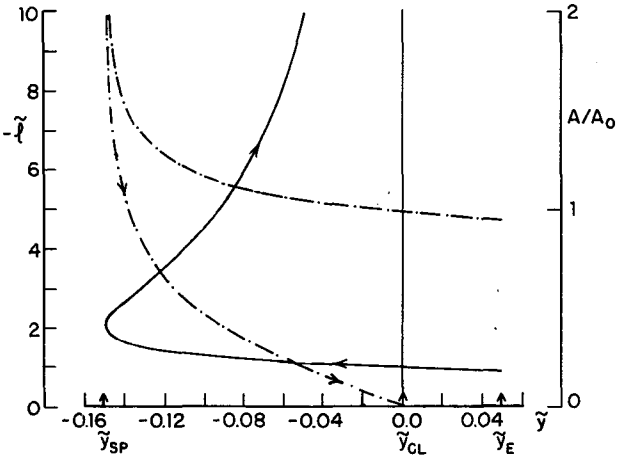

FIG. 4. As in Fig. 1 except for the southward traveling wave in a linearly opposing meridional flow with $\alpha = -1.0$.

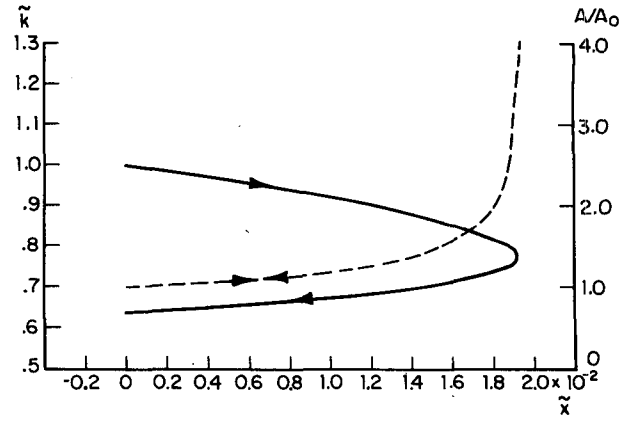

FIG. 5. As in Fig. 1 except for the eastward traveling wave in a linearly divergent flow.

3. The confluent jet

Observations of Rossby waves in constant zonal jets often show an aspect ratio $k/l \sim 1.0$ so that the zonal group velocity is approximately that of the jet. When such a wave encounters a region of increasing zonal velocity so that its zonal wavenumber k decreases, the group velocity also decreases causing the wave to reach a stopping point and its amplitude to increase. As an example of this we take $\tilde{k}_0' = 1.0$, $l_0' = 0.8$ and $\bar{U} = sx$. Figure 5 shows the wave excited at $\tilde{x} = 0.0$, reaching a stopping point at $\tilde{x} = 0.0195$ and then being reflected. The amplitude is seen to increase on approaching the stopping point. Such behavior of wave packets encountering divergent zonal velocity may be seen in the cold air outbreaks of the Western Pacific (Joung and Hitchman, 1984).

4. Energetics

The energy equation for barotropic Rossby waves (Young and Rhines, 1980) is

$$\frac{\partial E}{\partial t} + \nabla\cdot(\mathbf{C}E) = 2E\frac{K_iK_j}{K^2}\left(\bar{V}_{i,j} - \frac{1}{2}\delta_{ij}\nabla\cdot\bar{\mathbf{V}}\right),$$

where $\mathbf{C} = \bar{\mathbf{V}} + \mathbf{C}_g$, $K = (k, l)$ and i, j refers to the x and y component, respectively.

For waves in opposing zonal currents the variation of energy density of a wave packet is

$$\frac{\partial E}{\partial t} + \frac{\partial}{\partial x}(CE) = E\bar{U}_x\frac{k^2 - l^2}{k^2 + l^2}.$$

Integrating over a volume which contains the wave packet, we see that energy is gained as long as $l > k$ but due to the increase of k, eventually the wave energy is lost to the mean through the Reynold's stress. Sim-

ilarly for opposing meridional currents we find

$$\frac{\partial E}{\partial t} + \frac{\partial}{\partial y}(CE) = E\bar{V}_y \frac{l^2 - k^2}{k^2 + l^2}.$$

Again the increase in l results in an eventual loss of wave energy to the mean flow. The wave/mean flow problem will not be solved here, but we note that energy conservation requires the back effect of the dissipating waves on the flow is to accelerate it. This may, for instance, make the Hadley cell an effective "hydraulic breakwater" which absorbs wave energy while maintaining itself against dissipation in the process. In a zonal jet, regions where the wave is growing will be decelerated, the effect of these two processes in the presence of a background flow being to propagate the jet maximum downstream.

A more complete treatment of the energetics may be found in Hoskins *et al.* (1983). A two-dimensional model which illustrates the wave/mean interaction both in the linear and nonlinear case is presented by Shutts (1983).

5. Maintenance of diffluent jets

The formalism presented above envisions a wave source at x_E giving rise to an incoming wave which is reflected at x_{SP}. In the case of a diffluent jet, such as that occurring over the central North Pacific or central North Atlantic or the North Atlantic extension of the Gulf Stream, for that matter, we may envisage a spectrum of disturbances being swept along by the stream. In this case, greater realism results from adding a constant mean velocity to our divergent flow which simply translates the result. The component of this wave spectrum which corresponds to waves with group velocity opposing the current will be swept only to their respective stopping points where the decreasing zonal current equals their group velocity. From this point on, they will follow the reflected branch of our solution, losing energy to the mean as they approach x_{CL}. This dynamic interaction would maintain and perhaps build the jet outward as the waves dissipate. A diagnostic study of the diffluent region would reveal its being maintained at the expense of the waves.

As an additional illustration of this idea, we take the case of a wave with $\tilde{k}_0 = 1.0$, $\tilde{l}_0 = 0.0$ excited by topography at $\tilde{x}_E = -1.0$ so that $\omega = 0.0$. The resulting trajectory for $\bar{U} = -sx$ is shown in Fig. 6. Wavelength increases rapidly on approach to the critical level at $\tilde{x} = 0.0$ where the wave amplitude vanishes. Wave energy is lost to the mean flow all along this trajectory.

6. Shear line formation and the breakdown of zonal flows

Consider the quasi-stationary long waves in the 500 mb flow. Downstream of the 500 mb ridge typical convergences are $\sim 10^{-6}$ s^{-1} (Palmen and Newton, 1969)

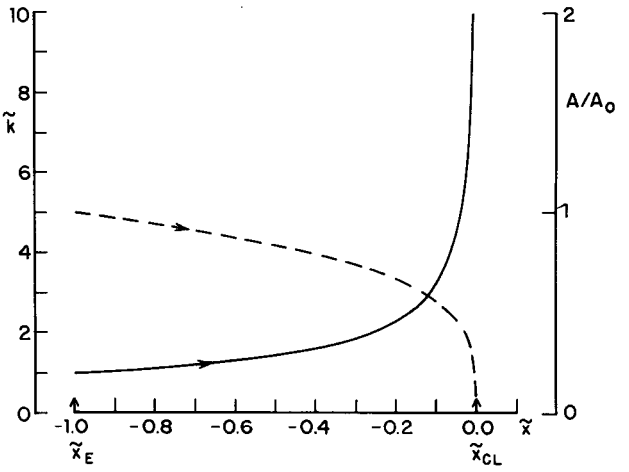

FIG. 6. As in Fig. 1 except for the wave excited by topography at $\tilde{x} = -1.0$.

which is of a magnitude to stop the embedded short waves that are steered by this flow. Such ridges are often found upstream of the central United States and western Europe, and the short waves which are steered by them would follow the trajectory of Fig. 2 with the addition of some mean translation. The increase in wavenumber by a factor ~ 2 as the wave amplitude and local vorticity increase owing to convergence, and the subsequent rapid increase in k, would look to the observer like an upper level cyclogenesis followed by the formation of a rapidly tightening upper level shear line (Halopainen and Rontu, 1981; Illari *et al.*, 1981). In the quite common situation of an equatorward mean flow in the convergent region, as between the 500 mb ridge and trough, the amplitude is additionally augmented by the source term in the wave action.

The essential contribution here is a focus on the convergent group velocity of the Rossby wave that forms the shear line rather than on the direct frontogenetic convergence of parcel trajectories, placing the theory of upper level shear line formations in the general theory of Rossby wave dynamics. We note that this mechanism is distinct from the one that gives rise to upper level fronts in developing baroclinic waves (Heckley and Hoskins, 1982).

A Rossby wave is made extremely vulnerable to convergent flow by becoming involved in a trajectory such as that of Figs. 1 and 2. On encountering convergence of as little as 10^{-6} s^{-1} over 4000 km, the wave is essentially destroyed by the inexorable increase of k. As a practical matter, Rossby waves are unable to penetrate such convergent flows and these flows act effectively as filters to Rossby waves entering them, much like the hydraulic breakwater in surface gravity wave theory. This cleaning out of the upper level waves may have an influence on the spectrum both spatially and in global average.

A series of waves entering a diffluent region over Western Europe has been carefully examined by Berg-

gren *et al.* (1949). These authors essentially suggest, qualitatively, the mechanism of Figs. 1 and 2, in an attempt to explain the observations.

7. Relation to cyclogenesis

We have pointed out that the rapid increase in amplitude and local vorticity of the upper level wave as it approaches its stopping point would be interpreted by an observer as an upper level cyclogenesis. Such episodic growth is characteristic of observed cyclogenesis which seldom displays the regular exponential increase in amplitude expected from eigenfunction analysis.

Surface cyclogenesis has recently been related theoretically to the presence of short waves aloft (Farrell, 1984). The above analysis suggests that preferred regions for the formation of such rapidly growing baroclinic waves should be under diffluent flows as the upper level wave is conditioned to take part in the process both by virtue of the increase in its amplitude and by the decrease in wavelength to a scale commensurate with typical surface depression. The relation of diffluence to cyclogenesis has long been recognized by synopticians (Palmen and Newton, 1969, p. 342 ff) and Bjerknes (1954).

8. Model results

To test these ideas, the equations for topographically forced barotropic Rossby waves on a sphere are solved in the presence of an opposing meridional current which crudely models the Hadley circulation.

The meridional propagation of Rossby waves on a sphere has been considered recently by Schneider and Watterson (1984). The waves were linearized perturbations of a zonal mean basic state satisfying the shallow water equations. If the basic state included a meridional flow $\bar{V}$ it was found that waves could propagate through easterlies if $\bar{V}$ was in the direction of propagation. The nondivergent dispersion relation was used to explain this propagation. Here it will be shown that a $\bar{V}$ in the opposite direction also significantly changes the wave behavior. Initial experiments were done with the shallow water model but in order to confirm the use of the nondivergent dispersion relation, and to allow more flexibility of numerical method, the solutions presented will be for the nondivergent vorticity equation on a sphere. The shallow water model showed similar behavior.

The barotropic vorticity equations for a layer of fluid on a sphere may be written

$$\frac{D\zeta}{Dt} = -\zeta \nabla \cdot \mathbf{v} + S,$$

where

$$\frac{D}{Dt} = \frac{\partial}{\partial t} + \frac{u}{a(1-y^2)^{1/2}}\frac{\partial}{\partial \lambda} + \frac{v(1-y^2)^{1/2}}{a}\frac{\partial}{\partial y},$$

ζ is the absolute vorticity,

$$\zeta = \frac{1}{a(1-y^2)^{1/2}}\frac{\partial v}{\partial \lambda} - \frac{1}{a}\frac{\partial}{\partial y}[u(1-y^2)^{1/2}] + 2\Omega y$$

a = the radius of the sphere
y = sin θ where θ is the latitude
λ = longitude
$\mathbf{v}$ = (u, v) the eastward and northward velocities respectively

and

$$\nabla \cdot \mathbf{v} \equiv \frac{1}{a(1-y^2)^{1/2}}\frac{\partial u}{\partial \lambda} + \frac{1}{a}\frac{\partial}{\partial y}[(1-y^2)^{1/2}v]$$ is the divergence.

The final term S represents vorticity sources and sinks, including those due to topography, heating and damping. We assume that a divergent basic state $[\bar{U}(y), \bar{V}(y)]$ may be balanced by $\bar{S}$ which is independent of nondivergent wave perturbations with velocity (u', v') generated by S'.

Linearizing about the basic state gives

$$\frac{\partial}{\partial t}\zeta' + \frac{\bar{u}}{a(1-y^2)^{1/2}}\frac{\partial}{\partial \lambda}\zeta' + \frac{1}{a}\frac{\partial}{\partial y}((1-y^2)^{1/2}\bar{v}\zeta') + v'\frac{(1-y^2)^{1/2}}{a}\bar{\zeta}_y = S',$$

where

$$\zeta' = \frac{1}{a^2}\left[\frac{1}{(1-y^2)}\frac{\partial^2}{\partial \lambda^2}\psi + \frac{\partial}{\partial y}\left((1-y^2)\frac{\partial \psi}{\partial y}\right)\right],$$

$$u' = -\frac{(1-y^2)^{1/2}}{a}\frac{\partial}{\partial y}\psi', \quad v' = \frac{1}{a(1-y^2)^{1/2}}\frac{\partial}{\partial \lambda}\psi'.$$

The perturbation quantities are assumed to be of the form

$$\psi' = \mathrm{Re}[e^{ik\lambda}\psi]$$

where

$$\psi = \psi_r(y) + i\psi_i(y).$$

The resulting ordinary differential equations in the variables ψ_r and ψ_i were finite differenced on 801 points equally spaced in y from -1 to $+1$. Solutions were obtained using a library inversion routine.

The equation for ψ is, in fact, singular at the critical points where $\bar{V}$ becomes zero, or at $\bar{U} = 0$ in the case where $\bar{V}$ is zero everywhere. While an Ekman damping $D\zeta'$ was found to be adequate to obtain meaningful solutions, there remained slight noise in the vorticity which only slowly disappeared as resolution was increased. Introducing a small viscous-like term $d^4\psi/dy^4$ in the neighborhood of the $\bar{V} = 0$ points was adequate to remove the noise and resolve the singularities. Since the linear damping only then serves to damp the waves, it was omitted in the cases shown.

The basic states and forcings were chosen to show the wave turnaround produced by an opposing current. The forms of $\bar{U}$ and $\bar{V}$ are illustrated in SW.

In both cases presented, the following values are taken

$$a = 6.371 \times 10^6 \text{ m},$$

$$\Omega = 7.292 \times 10^{-5} \text{ s}^{-1},$$

$$\bar{U}(y) = 15 \sin\left(\frac{3\pi}{2}(1 + y)\right) + 18(1 - y^2).$$

The forcing is in the form of a divergence with wavenumber $k = 3$, as might be produced by heating or topography in the atmosphere

$$S' = \begin{cases} \text{Re}\left\{0.3 \times 10^{-7} \bar{\zeta} e^{i3\lambda} \times \cos\left[\frac{\pi}{10^\circ}(\theta - 45^\circ)\right]\right\} \\ \qquad\qquad \text{for} \quad 40^\circ < \theta < 50^\circ \\ 0, \quad \text{elsewhere.} \end{cases}$$

Figure 7 shows the amplitude and phase of the streamfunction ψ' and the zonal wind u' as a function of latitude for the case $\bar{V} = 0$ everywhere. Note that for ψ, amplitude is $(\psi_r^2 + \psi_i^2)^{1/2}$ and phase is $\tan^{-1}(\psi_i/\psi_r)$. Since there are no easterlies the wave propagates

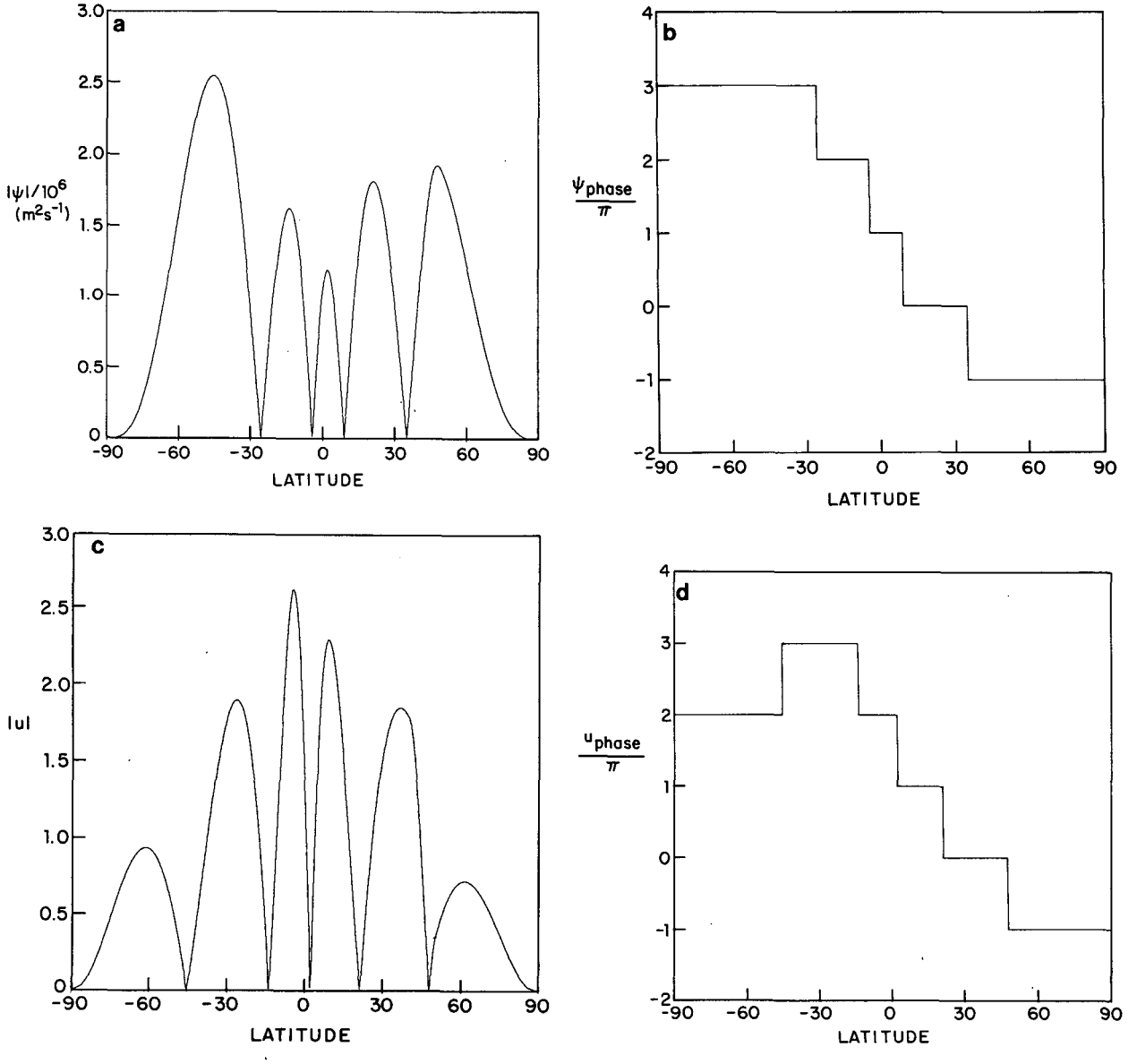

FIG. 7. Meridional structure of perturbation solution for $\bar{V} \equiv 0$. (a) Amplitude, (b) phase of ψ, (c) amplitude and (d) phase of u.

through to the other hemisphere and no critical points are encountered.

The introduction of the meridional wind $\bar{V} = V_1$ where

$$V_1(y) = \begin{cases} 0.8 \sin\left(\pi \dfrac{y + 0.3}{0.2}\right), & -0.5 \leqslant y \leqslant -0.3 \\ 3.2 \sin\left(\pi \dfrac{y + 0.3}{0.8}\right), & -0.3 \leqslant y \leqslant 0.5 \\ 0, & |y| > 0.5, \end{cases}$$

produces the solution shown in Fig. 8. Marked on the graphs are the stopping point *SP* and critical point *CL* as discussed in Section 2.

Following Karoly (1983) the WKB approximate solution is obtained in the nondimensional Mercator coordinate form of the vorticity equation and, as in Schneider and Watson (1984), the relevant roots of the dispersion relation, l, and the corresponding meridional group velocities are shown as functions of latitude in Fig. 9. The southward propagation of the waves of the branch marked *I* is halted by the opposing flow

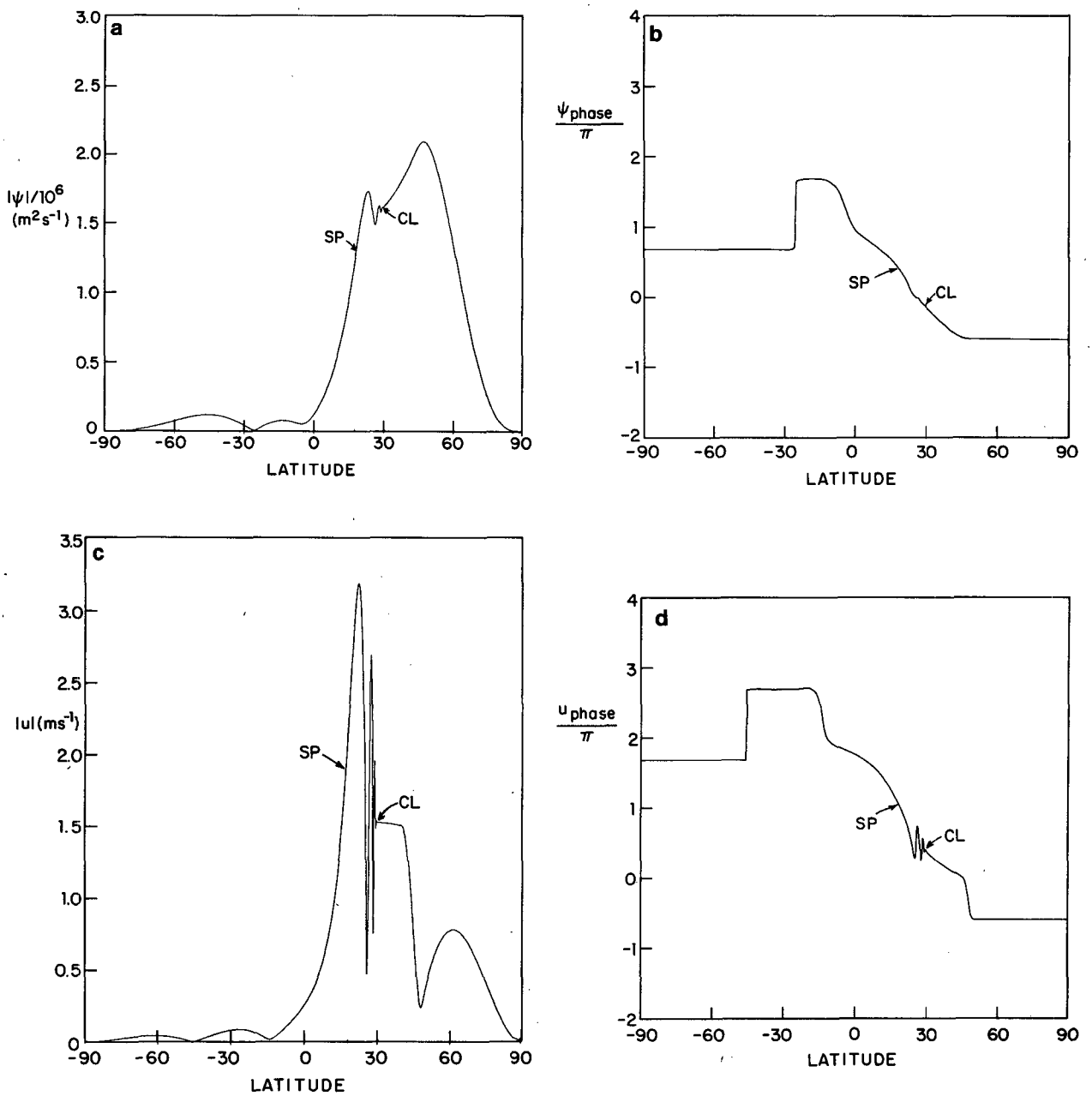

FIG. 8. As in Fig. 7 but for $\bar{V} = V_1$. *SP* denotes stopping point, *CL* denotes critical latitude.

$\bar{V}$ at 18°N. The roots behave as $l - l_s \sim (y_M - y_s)^{1/2}$ close to the stopping point y_s as shown in Section 2. The turnaround of wave energy onto a wave train with the wavenumber branch marked *II* is evidenced by the short wavelength oscillation in the graphs between 18 and 30°N. Although the amplitude of this slowly northward propagating wave diminishes as the critical point is approached, its wavenumber increases and hence the oscillations in $|u| \sim l|\psi|$ are much greater than those in $|\psi|$. The vorticity (not shown) is dominated by the large wavenumber component and its amplitude reaches large values near 30°N with little oscillation. The wave amplitude south of 18°N is dramatically reduced by the opposing flow. In the asymptotic limit

$$\frac{d\bar{U}}{dy_M}(l\bar{U})^{-1} \to 0,$$

the solution is $\psi \sim A_i(y_M - y_s)\exp[il_s(y_M - y_s)]$, where A_i is the Airy function, with an equal amplitude of return wave as incoming wave near the stopping point.

In Fig. 8 the wavelength at the stopping point is comparable to the length scale of the basic state variation but $|\psi|$ still resembles A_i near *SP* and there is an appreciable return wave.

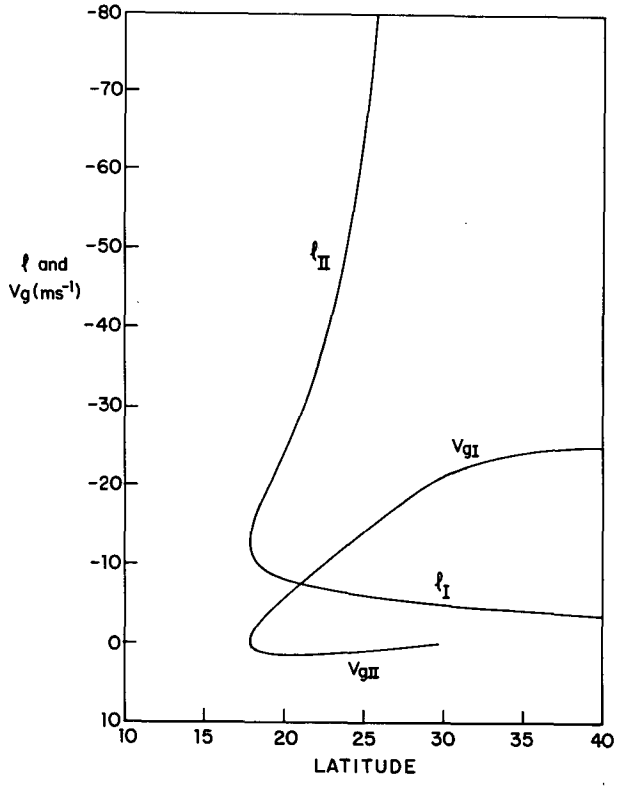

FIG. 9. Meridional wavenumber for the nondimensional Mercator coordinate and corresponding meridional group velocity in m s^{-1} as a function of latitude. Incoming wave branch is denoted by *I* and the return branch by *II*. Note that the same inverted scale serves both quantities.

It may be relevant to diagnostic studies of short atmospheric waves that the shortwave component appears here near the $\bar{V} = 0$ point at 30°. A $\bar{U} = 0$ critical line is not required to produce short waves. Indeed none appear at $\bar{U} = 0$ in the case where an easterly band is present near the equator since with $\bar{V} \neq 0$ there is no critical line at $\bar{U} = 0$.

9. Conclusions

Although this study is far from complete, it has shown that Rossby waves in divergent and convergent flows are rich in their dynamics. Cyclogenesis due to zonal variation of the zonal velocity may be as important in the atmosphere as the more familiar growth of perturbations in shear and likely to be complementary. The vulnerability of waves in convergent flow is shown to filter them and, in the process, result in the formation of shear lines with implications for the local and global wave spectrum. Examples of zonal flow breakdown are related to the growth in amplitude and to the back effect of wave/mean flow interaction.

Among the limitations of this study is the use of the WKB approximation which we have addressed by showing that qualitative predictions are robust in a model where scale separation is violated. Other limitations include the restriction to barotropic waves, while observation suggests that the third dimension becomes important as the steepness increases and the assumption of a divergent flow. It is likely that a baroclinic shear flow would permit greater realism and perhaps the formation of closed vortices.

Acknowledgment. This work was supported by NASA Grant NGL 22-007-228.

REFERENCES

Berggren, R., B. Bolin and C. G. Rossby, 1949: An aerological study of zonal motion, its perturbation and breakdown. *Tellus,* **1,** 14–37.

Bjerknes, J., 1954: The diffluent upper trough. *Arch. Meteor. Geophys. Bioklim.,* **A7,** 41–46.

Dickinson, R. E., 1968: Planetary Rossby waves propagating vertically thorugh weak westerly wind wave guides. *J. Atmos. Sci.,* **25,** 984–1002.

Farrell, B., 1984: Modal and non-modal baroclinic waves. *J. Atmos. Sci.,* **41,** 668–673.

Geisler, J. E., and R. E. Dickinson, 1974: Numerical study of an interacting Rossby wave and barotropic zonal flow near a critical level. *J. Atmos. Sci.,* **31,** 946–955.

——, and ——, 1976: Critical level absorption of barotropic Rossby waves in a north–south flow. *J. Geophys. Res.,* **27,** 3805–3811.

Heckley, W. A., and B. J. Hoskins, 1982: Baroclinic waves and frontogenesis in a non-uniform potential vorticity semi-geostrophic model. *J. Atmos. Sci.,* **39,** 1999–2016.

Holopainen, E. O., and L. Rontu, 1981: On shear lines in the upper troposphere over Europe. *Tellus,* **33,** 351–359.

Hoskins, B., I. James and G. White, 1983: The shape, propagation and mean-flow interaction of large scale weather systems. *J. Atmos. Sci.,* **40,** 1595–1612.

Illari, L., P. Malguzzi and A. Speranza, 1981: On breakdown of the westerlies. *Geophys. Astrophys. Fluid Dyn.*, **17**, 27–49.

Joung, C. H., and M. Hitchman, 1984: On the role of successive downstream development in East Asian polar air outbreaks. *Mon. Wea. Rev.*, **110**, 1224–1237.

Karoly, E. K., 1983: Rossby wave propagation in a barotropic atmosphere. *Dyn. Atmos. Oceans*, **7**, 111–125.

Lighthill, J., 1978: *Waves in Fluids*, Cambridge University Press, 504 pp.

Palmen, E., and C. W. Newton, 1969: *Atmospheric Circulation Systems*, Academic Press, 603 pp.

Peregrine, D. H., and R. Smith, 1979: Nonlinear effects upon waves near caustics. *Phil. Trans. Roy. Soc. London*, **A292**, 341–370.

Schneider, E. K., and I. G. Watterson, 1984: Stationary Rossby wave propagation through easterly layers. *J. Atmos. Sci.*, **41**, 2069–2083.

Shapiro, L. J., 1977: Tropical storm formation from easterly waves: A criterion for development. *J. Atmos. Sci.*, **34**, 1007–1021.

Shutts, G. J., 1983: The propagation of eddies in diffluent jetstreams: Eddy vorticity forcing of blocking fields. *Quart. J. Roy. Meteor. Soc.*, **109**, 737–761.

Smith, R., 1976: Giant waves. *J. Fluid Mech.*, **77**, 417–431.

——, 1980:

Tung, K. K., 1979: A theory of stationary long waves. Part III: Quasi normal modes in a singular waveguide. *Mon. Wea. Rev.*, **107**, 751–774.

Yamagata, T., 1976: On trajectories of Rossby wave-packets released in a lateral shear flow. *J. Oceanogr. Soc. Japan*, **32**, 162–168.

Young, W. R., and P. B. Rhines, 1980: Rossby wave action, enstrophy and energy in forced mean flows. *Geophys. Astrophys. Fluid Dyn.*, **15**, 39–52.